



# **SHocks: structure, AcceleRation, dissiPation**

Work Package 4  
Exploring acceleration in astrophysical shocks  
through broadband emission

Deliverable D4.2  
Technical report on the application of model to  
X-ray data

Emanuele Greco<sup>1</sup>, Jacco Vink<sup>1</sup> Amael Ellien<sup>1</sup>

<sup>1</sup> Anton Pannekoek Instituut/GRAPPA, University of Amsterdam, Science Park  
904, 1098 XH Amsterdam, The Netherlands

26/04/2022

This project has received funding from the European Union's Horizon 2020  
research and innovation programme under grant agreement No 101004131



## Document Change Record

Issue	Date	Author	Details
1.0	22.04.2022	E. Greco	Initial draft
1.1	26.04.2022	E. Greco	Final draft

## Table of Contents

<b>1</b>	<b>Summary</b>	<b>3</b>
<b>2</b>	<b>Introduction</b>	<b>3</b>
<b>3</b>	<b>NuSTAR, INTEGRAL and SWIFT analysis</b>	<b>4</b>
3.1	Image analysis	4
3.2	Spectral analysis	5
<b>4</b>	<b>Next steps: spatially resolved spectral analysis and inclusion of Chandra data</b>	<b>8</b>
<b>5</b>	<b>Conclusion</b>	<b>8</b>
<b>6</b>	<b>References</b>	<b>9</b>

## 1 Summary

X-ray emission from young supernova remnants (SNRs) is characterized by non-thermal radiation caused by the synchrotron process. This type of emission is usually detected in regions close to the shock front and it is observed to extend till energy of  $\sim 100$  keV. The up-to-date theory to explain the observed synchrotron radiation is based on the diffusive shock acceleration (DSA), which requires high magnetic turbulence. However, the current spectral models used to fit the data overlook the influence of the turbulence in the shape of the spectrum itself.

We developed a spectral model that takes into account the effect of the magnetic turbulence on the shape of the X-ray spectra. This model can be called within the XSPEC, the most popular X-ray analysis software.

We report on the X-ray analysis of spectra extracted from the young SNR Cassiopeia A (Cas A), comparing different spectral models and discussing the implications. The spectral analysis show that a simple power-law is best suited to describe the observations and, therefore, jitter model can be invoked as a convincing radiation mechanism.

## 2 Introduction

The aim of the project is to apply the models explained in technical report D4.1 and apply them to hard X-ray data from young SNRs. The implication of these models is that they provide a window onto the magnetic-field turbulence spectrum within the emitting SNR plasmas. We refer to Deliverable 4.1 for a full introduction and contextualization of this work, and we just recall the main highlights. Synchrotron radiation in a turbulent magnetic field leads to a power-law component which can extend, in principle, till gamma-ray energies (Kelner et al., 2013). The synchrotron radiation in a turbulent magnetic field is often called *jitter radiation*. Most promising targets for detection of the jitter radiation are young SNRs, characterized by high signal-to-noise ratio in the energy band above 10 keV. Among the possible sources, we focused on Cas A which is one the brightest SNR and show clear emission at least up to 100 keV.

The typical spectral model used up to now to describe the X-ray synchrotron radiation in SNRs are based on a power-law component, which can also be shaped by an exponential cut-off:

$$n(h\nu) \propto (h\nu)^{-\Gamma} \exp \left[ - \left( \frac{h\nu}{h\nu_c} \right)^\beta \right] \quad (1)$$

where  $\Gamma$  is the spectral photon index,  $h\nu$  is the energy,  $h\nu_c$  is the cut-off energy and  $\beta$  a factor which shapes the cut-off. In the so-called age-limited scenario (Reynolds, 1998),  $\beta = 1$  and the corresponding spectral model within XSPEC is `srcut` (Reynolds & Keohane, 1999). In the loss-limited scenario (Zirakashvili & Aharonian, 2007),  $\Gamma$  is expected to be steeper and  $\beta = 0.5$ . The latter scenario does not have a corresponding spectral model within XSPEC. Therefore, we defined a model `zira` in XSPEC, using the analytical expression given by Eq. 37 in Zirakashvili & Aharonian (2007). Both these models do not take into account the effects of magnetic-field turbulence, although the cutoff energy itself can usually only be reached if magnetic-field turbulence is substantial ( $\delta B/B \sim 1-10$ ). As

already discussed in Deliverable 4.1, we also consider the `jitter` model, that is now implemented also in the non-python version of XSPEC.

### 3 NuSTAR, INTEGRAL and SWIFT analysis

Table 1: Observation log table

Telescope	Obs ID	PI	Exposure Time (ks)
NuSTAR	40001019002	Harrison	294
	40021002002	Harrison	288
	40021011002	Harrison	246
	40021012002	Harrison	239
	40021003003	Harrison	233
	40021001005	Harrison	228
	40021002008	Harrison	226
	40021001002	Harrison	190
	40021015003	Harrison	160
	40021002006	Harrison	159
	40021015002	Harrison	86

We considered archival X-ray observations performed by detectors sensitive to energies  $\geq 10$  keV: *NuSTAR*/FPMA,B, *INTEGRAL*/ISGRI and *Swift*/BAT. The only telescope with spatial resolution good enough to resolve Cas A in this spectral band is *NuSTAR*, which employs Wolter type X-ray telescopes, whilst both *INTEGRAL* and *Swift* are coded mask instruments, for which source localization is achieved through the shadowing casts by the pattern of a metal plate (coded mask) with a particular pattern. Code masks do not allow for a direct imaging of an X-ray source, and only the spectrum of the source can be extracted, and the source, i.e. Cas A, is treated as a point source. The disadvantage of *NuSTAR* is that the maximum photon energy it can detect are  $\sim 80$  keV, whereas *INTEGRAL*/ISGRI and *Swift*/BAT have sensitivities to much higher energies, although for Cas A the statistics above 100 keV is poor. Details of the *NuSTAR* observations are reported in Table 1. Data reduction and analysis of *NuSTAR* data are performed using the standard tasks `nupipeline` and `nuproducts` available within the software NuSTARDAS. *INTEGRAL*/ISGRI spectra are obtained through the MMODA website (Neronov et al., 2021). *Swift*/BAT spectra can be found online at SWIFT/BAT-CasA.

#### 3.1 Image analysis

We produced vignetting-corrected count-rate *NuSTAR* images of Cas A in various energy bands, in order to look for potential variation in the surface brightness of the remnant at different wavelengths and to check in what energy band the background emission is comparable with the signal of Cas A. The resulting images are shown in Fig. 1.

We also produced analogous maps, corrected by the *NuSTAR* point-spread-function (PSF) through the Lucy-Richardson algorithm (Lucy, 1974; Richardson,

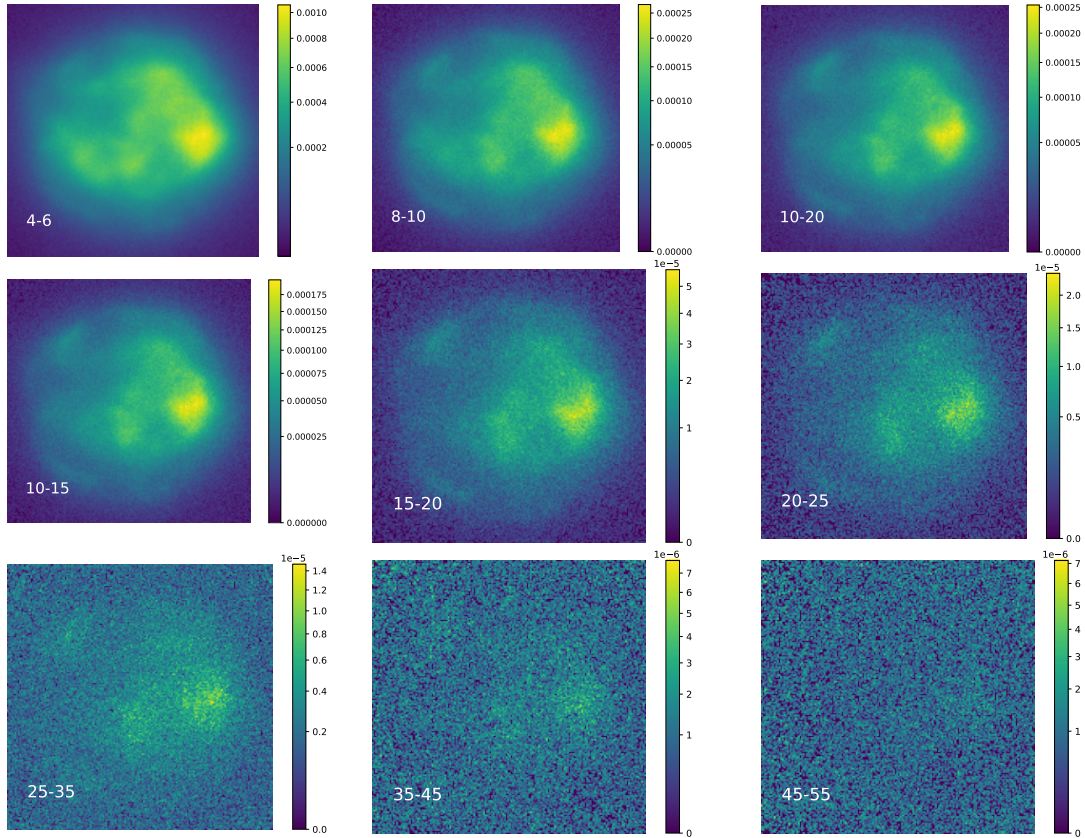


Figure 1: Exposure/vignetting-corrected and mosaicked *NuSTAR* image of Cas A in various energy bands, expressed in keV

1972). Such images, shown in Fig. 2 provide a better view of the plasma distribution. In particular, a region in the western part of Cas A is particularly bright in every energy band.

Fig. 1 and 2 are also relevant in the perspective of performing a spatially resolved analysis of the hard non-thermal X-ray emission observed in Cas A. In fact, we plan to extract spectra from different regions of Cas A, to check whether the jitter radiation is detectable all over the remnant, if it is confined to smaller areas or its spectral characteristics differ from region to region.

As mentioned above, *NuSTAR* is the only X-ray telescope sensitive to energies higher than 10 keV able to spatially resolve Cas A. Simultaneous analysis of *NuSTAR*/FPMA,B, *INTEGRAL*/ISGRI and *Swift*/BAT spectra can be done only considering the whole Cas A emission, as we discuss in the next section.

### 3.2 Spectral analysis

We simultaneously fitted *NuSTAR*, *INTEGRAL* and *Swift* data of Cas A adopting various setups and models.

We excluded from the analysis spectral channels at energy lower than 15 keV. This is done because we expect that the thermal emission, due to shock-heated plasma, is not negligible below this energy threshold and, therefore, might cause a misleading interpretation of the spectra. We only consider spectral bins where the background emission is a small fraction ( $< 10\%$ ) of the Cas A emission. This means that the *NuSTAR* data are included till energy of 40 keV, the *INTEGRAL*

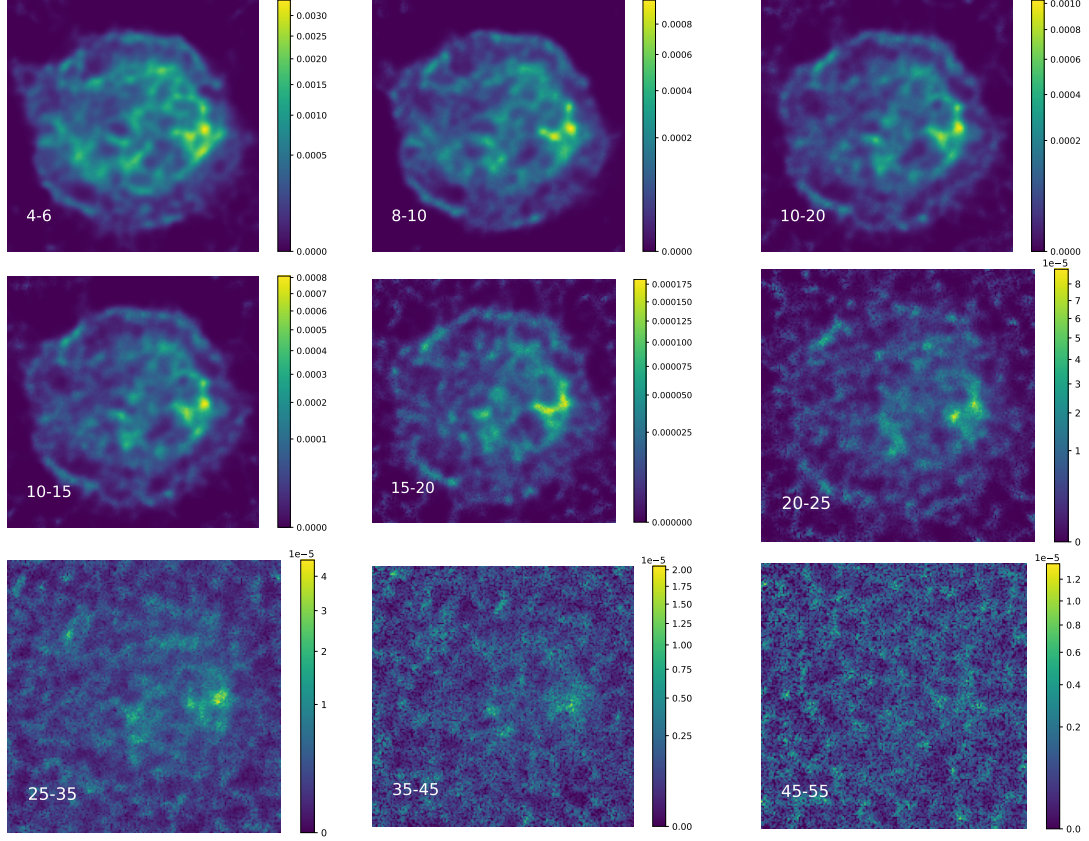


Figure 2: Deconvolved, exposure/vignetting-corrected and mosaicked *NuSTAR* image of Cas A in various energy bands, expressed in keV

data between 40 keV and 100 keV<sup>1</sup> and the *Swift* data between 15 keV and 200 keV.

Since *NuSTAR* is characterized by two detectors, we have a total of 22 *NuSTAR* spectra. We performed the analysis either by summing these *NuSTAR* spectra and by simultaneously fitting each of them extracted from the 11 *NuSTAR* observations. These two slightly different approach have pro and cons which balance each other out. Summing the spectra leads to a single global spectrum with much higher statistics, smaller error bars and, therefore, to higher sensitivity to the spectral model adopted. However, given that there are 11 separate *NuSTAR* observations being the 11 *NuSTAR* observations performed in a time-lapse of 2 years (see Table 1), the response matrix and the physical characteristics of the plasma might slightly change between the first and the last observations, possibly causing misleading results. On the other hand, the simultaneous analysis of the single spectra extracted from each observation, provide very reliable results, at the expense of the sensitivity to the spectral model.

With the above consideration in mind, we first adopted the most conservative setup, by simultaneously fitting each single *NuSTAR* spectrum together with the *INTEGRAL* and *Swift* ones. We adopt the three spectral models introduced in report D4.1 and that have been used in literature to fit the X-ray synchrotron spectra of SNRS: `power-law`, `srcut` and `zira`. We also include the `jitter` model, whose development and physical ratio can be found in Deliverable 4.1. Each of

<sup>1</sup>*INTEGRAL*/ISGRI data below 40 keV are excluded for known calibration issues

this model is coupled to a component taking into account the Galactic absorption (TBabs model in XSPEC) and to two gaussians, which account for the radioactive  $^{44}\text{Ti}$  associated lines observed in Cas A at 65 keV and 82 keV (e.g., Grefenstette et al., 2014). Values of  $\chi^2$  for each adopted model are shown in Table 2. Fig. 3 show the *NuSTAR*, *INTEGRAL* and *Swift* spectra fitted with the different models and the corresponding residuals.

NuSTAR simultaneous + ISGRI + SWIFT	
Zira	2384/1843
Srcut	2267/1844
Power-law	2174/1843
Jitter	2179/1842
NuSTAR combined + ISGRI + SWIFT	
Zira	280/116
Srcut	189/117
Power-law	129/116
Jitter	129/115

Table 2:  $\chi^2/\text{d.o.f.}$  values for different spectral models adopted in the 15-100 keV band

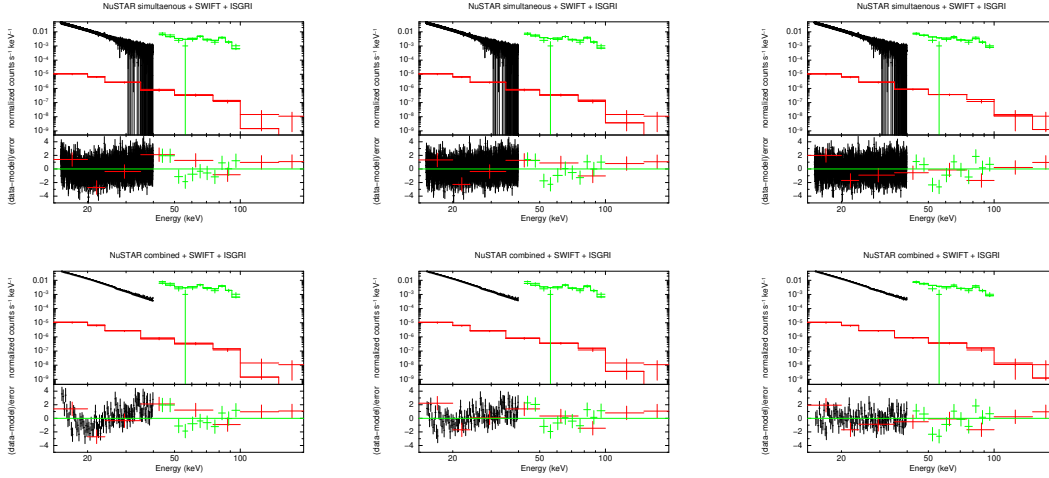


Figure 3: *NuSTAR*, *INTEGRAL* and *Swift* spectra of Cas A fitted with different models. *From left to right*: spectra are fitted with the *zira*, *srcut* and *pow/jitter* model, respectively (*jitter* model provides same description as the *pow*). *Upper panels*. *NuSTAR* spectra from all the observations are simultaenously fitted. *Lower panels*. *NuSTAR* spectra from all the observations are combined.

As can be easily seen by looking both at residuals in Fig. 3 and at the  $\chi^2$  values of Table 2, the model best reproducing the hard X-ray spectra of Cas A is a simple power-law. The models including an exponential cut-off, *zira* and *srcut*, lead to strong residuals, indicating that there is no hint for such a cut-off in the spectra. The *jitter* model provides same results as the single power-law, with a best-fit photon index  $\Gamma \sim 3.3$ . Therefore, it is natural to interpret the best-fit power-law as the harder component of the jitter radiation, indicating that the lower energy component is not detectable in the energy range considered (see Sect. 4)

As discussed in the Deliverable 4.1, in the `jitter` scenario, the photon index  $\Gamma$  of the power-law is directly linked to the power-law index  $\alpha$  of the turbulence spectrum through the relation  $\Gamma = \alpha + 1$ . Therefore, we have  $\alpha = 2.3$ , which is comparable to the Bohm diffusion scenario ( $\alpha = 2$ ).

Note that the recently submitted paper by Ellien, A. et al. on 0.5–10 keV spectra from Tycho’s SNR also indicated that a simple power-law model is preferred over `srcut`, which may also provide evidence for the jitter process in this remnant.

## 4 Next steps: spatially resolved spectral analysis and inclusion of Chandra data

In Sect. 3.2 we showed that the hard X-ray spectra of Cas A do not show any cutoff, at odds with what has been done in the literature to model synchrotron radiation (see Vink 2020 for a review). On the other hand, the continuum emission in the 15-100 keV band can be described with a single power-law, given that also the best-fit jitter model provides only one significant component. Assuming that the observed power-law is the jitter component, one could wonder why we did not observe the synchrotron component. One of the possible explanation is that that the latter is actually detectable at lower energies, either outside of the X-ray regime, or just at energy ranges not considered so far.

In order to address these issues, we are currently including *Chandra*/ACIS data in the analysis, in order to cover a wider energy range of the X-ray emission of Cas A. Since the emission below 10 keV is dominated by shocked-heated plasma, a more complex fit is required, including shock-heated plasma components (e.g., `vnei` model in XSPEC). By robustly constraining the thermal emission in the 0.5-8 keV band, we can also estimate the ratio of the non-thermal flux over the thermal one. This approach will also allow us to consider *NuSTAR* data points between 3 and 15 keV, which, so far, have been ignored to exclude potential thermal contaminations in the spectra.

Another advantage provided by the inclusion of the *Chandra*/ACIS spectra, is the possibility to perform a spatially resolved spectral analysis of the non-thermal component of Cas A in a range between 0.5 keV and 30 keV. In fact, both *Chandra* and *NuSTAR* can resolve Cas A, even though with different spatial resolution, allowing to probe the jitter scenario in different regions. In particular, a promising target is the Western part of Cas A, where both the *Chandra* (Hwang & Laming, 2012) and *NuSTAR* images show bright non-thermal emission.

## 5 Conclusion

In this technical report, we showed that the hard X-ray spectra of Cas A are best described by a simple power-law component. Considering more complex spectral models that rely on exponential cut-off leads to a significantly worse fit of the observed data. This result strongly indicates the jitter radiation is best suited to account for the observed emission and we measured a X-ray photon index  $\Gamma = 3.3$ , indicating a turbulence power-law index  $\alpha = 2.3$ , comparable to the

Bohm diffusion scenario. We also applied the jitter model, that we implemented in the XSPEC software, made of a low-energy component similar to the synchrotron radiation and an high-energy one which can be described by a power-law. The results obtained by using the jitter model are substantially indistinguishable from those obtained by using a simple power-law. This is most likely due to the fact that the energy range covered in the analysis is 15 to 100 keV, whilst the pre-break component might be detectable at lower energies, or could even be outside of the X-ray domain. This may have consequences for the inferred maximum electron cosmic-ray energies in Cas A. Our next step will be to include *Chandra* data in our analysis, in order to extend the analysis to lower energies ( $\sim 0.5$  keV) and to study the spatial distribution of the detected power-law. In addition, we would like to extent this analysis to the hard X-ray spectra from Tycho's SNR, Kepler's SNR and SN1006.

## 6 References

- Grefenstette, B. W., Harrison, F. A., Boggs, S. E., et al. 2014, , 506, 339, doi: 10.1038/nature12997
- Hwang, U., & Laming, J. M. 2012, , 746, 130, doi: 10.1088/0004-637X/746/2/130
- Kelner, S. R., Aharonian, F. A., & Khangulyan, D. 2013, , 774, 61, doi: 10.1088/0004-637X/774/1/61
- Lucy, L. B. 1974, , 79, 745, doi: 10.1086/111605
- Neronov, A., Savchenko, V., Tramacere, A., et al. 2021, , 651, A97, doi: 10.1051/0004-6361/202037850
- Reynolds, S. P. 1998, , 493, 375. [http://cdsads.u-strasbg.fr/cgi-bin/nph-bib\\_query?bibcode=1998ApJ...493..375R&db\\_key=AST](http://cdsads.u-strasbg.fr/cgi-bin/nph-bib_query?bibcode=1998ApJ...493..375R&db_key=AST)
- Reynolds, S. P., & Keohane, J. W. 1999, , 525, 368. [http://cdsads.u-strasbg.fr/cgi-bin/nph-bib\\_query?bibcode=1999ApJ...525..368R&db\\_key=AST](http://cdsads.u-strasbg.fr/cgi-bin/nph-bib_query?bibcode=1999ApJ...525..368R&db_key=AST)
- Richardson, W. H. 1972, *Journal of the Optical Society of America (1917-1983)*, 62, 55
- Vink, J. 2020, *Physics and Evolution of Supernova Remnants*, doi: 10.1007/978-3-030-55231-2
- Zirakashvili, V. N., & Aharonian, F. 2007, , 465, 695, doi: 10.1051/0004-6361:20066494